Chapter 11

Magma Ascent and Degassing at Shallow Levels

Alain Burgisser

CNRS, ISTerre, Le Bourget du Lac, France, Université de Savoie, ISTerre, Le Bourget du Lac, France

Wim Degruyter

School of Earth & Atmospheric Sciences, Georgia Institute of Technology, Atlanta, GA, USA

Chapter Outline

GLOSSARY

bubble Void space in a silicate melt that is filled by a gas phase. Bubbles are spherical unless deformed by stress or coalescence.

coalescence Process by which two or more bubbles merge into each other, forming a network through which gas can flow.

crystal Solid phase of a magma.

degassing General process by which magma loses its volatile elements. Degassing can occur by exsolution and/or by outgassing.

exsolution Process by which dissolved volatiles come out of solution to join a coexisting gas phase (generally present as bubbles).

melt Liquid phase of a magma.

microlite Small crystals (tens of micrometers across) occurring in magmas. They are generally formed during magma ascent as a consequence of volatile loss from the melt.

phenocrysts Large crystals (hundreds of micrometers across) occurring in magmas. They are generally inherited from the magmatic chamber.

outgassing Loss of the gas phase from a magma.

permeability (magmatic) A material property quantifying the resistance encountered by gas flowing through an interconnected network of bubbles.

rheology Physical description of the way magma deforms when under stress. It generally involves the property of viscosity.

saturation Maximum quantity of volatile element that can be dissolved in a silicate melt.

vesicle Void space left in a solidified magma. It could correspond to a bubble having lost its gas, or to stress-generated fractures.

vesicularity The ratio of void space to total magma volume. Also named porosity or gas volume fraction.

viscosity Material property linking the amount of deformation of a fluid to the amount of applied stress.

volatiles Chemical elements or species that preferentially partition into the gas phase of a magma.

1. GENERAL PRINCIPLES

The most dramatic change that magma undergoes while ascending to the surface is volatile loss because of pressure drop. The process by which the silicate melt loses its dissolved volatile is called degassing. It is the main mechanism by which magma can reach the volcanic vent either as a mostly degassed lava that oozes quietly or as a fragmented mixture of gases and particles that explosively rushes out into the atmosphere. Degassing causes gases to accumulate into the magma in the form of **bubbles** that transform the magma into foam. It causes some **crystals** to grow and the melt **viscosity** to increase. The appearance of bubbles and new crystals transforms the magma into an unstable mixture of liquid, crystals, and gas bubbles, which flows and reacts to stress in complex ways. Some of these

The Encyclopedia of Volcanoes. http://dx.doi.org/10.1016/B978-0-12-385938-9.00011-0

The Encyclopedia of Volcanoes, Second Edition, 2015, 225−236

changes occur at the submillimeter scale while others affect the entire plumbing system. The outcome of the impending volcanic eruption is most often controlled by the interactions between small- and large-scale processes rather than by one dominant length scale.

Small-scale magmatic processes that are important at shallow levels concern the three phases that make magma. The first phase, melt, contains dissolved **volatiles** that have evolving solubilities and that are regulated by chemical reactions. The second phase is composed of gas bubbles that successively nucleate, grow, and coalesce, possibly creating pathways for the gas to escape from the magma. The third phase is composed of crystals that also nucleate, grow, and may change shape during ascent. Each of these small-scale processes has been studied experimentally or theoretically in isolation of the others so as to yield a detailed vision of how degassing affects the three phases composing magma.

There are four main large-scale magmatic processes. One process is how magma as a whole (melt, bubbles, and crystals) flows under stress, which drove scientists to study its rheological properties. Another is how the geometry of the volcanic conduit influences magma ascent, which involves the characterization of the various plumbing systems feeding volcanoes. The third process is how the gas can escape out of the foamy magma, which brought forth the concept of **outgassing**. The last process involves the interactions between the magma-filled conduit and the rest of the volcanic edifice.

Both small- and large-scale processes interact in complex ways. Natural observations, whether of the actual eruption or its products, show an integrated result of all ascent-related processes. To understand the interactions between these processes, the most-often used tools are numerical models issued from fluid dynamics. Conduit flow models in particular are amenable to select a subset of small- and large-scale magmatic processes and to generate a general picture of the ascent regimes they sustain.

2. SMALL-SCALE PROCESSES

2.1. Chemistry of Volatile Loss

Silicate melts contain up to a few weight percent of dissolved volatiles. These volatiles, which involve elements, such as O, H, C, S, and halogens, such as F and Cl, are named so because they preferentially partition into the gas phase as opposed to the crystalline phase. Measures of volcanic gases emitted at the vent indicate that H_2O is the dominant gas, followed by CO_2, SO_2, and minor amounts of H_2S, CO, HCl, and HF. Figure 11.1 shows representative gas compositions for a basaltic melt at Etna and a rhyolitic melt at Mt St Helens. These high temperature gases were measured at the vent at atmospheric pressure. At depths, when the gas phase was

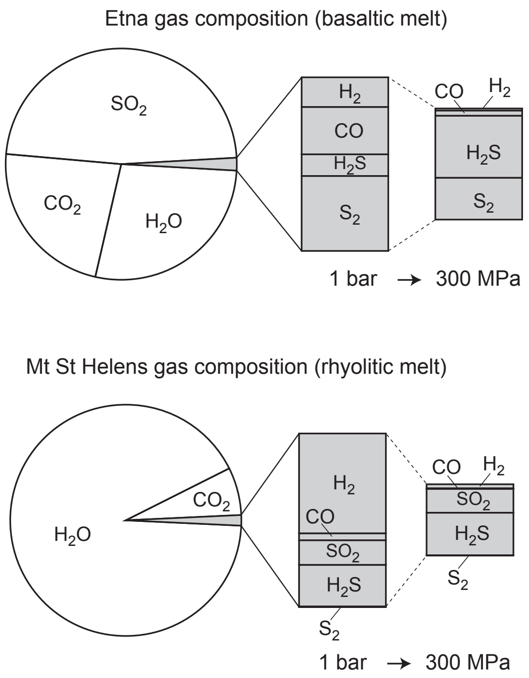

FIGURE 11.1 Representative compositions of volcanic gases emitted during eruptions involving basaltic and rhyolitic melts, respectively. Pie charts represent chemical species proportion with respect to 100% in molar fraction. Bar columns in the middle represent the molar proportions of minor species as measured at the vent (0.1 MPa). Bar columns on the right represent the molar proportions of minor species when the gas is compressed back to magma chamber levels (300 MPa) without interacting with the host melt. Recompression does not affect major species proportions in a visible manner, so pie charts at 300 MPa were omitted. *Data from Symonds et al. (1994) in Carroll and Holloway (1994).*

trapped into bubbles in the volcanic conduit or the magma chamber, these gases had different compositions for two reasons: first, because of the high temperature, there are fast chemical reactions within the gas itself that dictate the proportions of all present species. These reactions are sensitive to pressure, and so at a depth gas composition changes. These changes mostly affect minor species such as H_2S or CO (Figure 11.1). Second, another set of chemical reactions occur between the gaseous and the dissolved species. The maximum amount of volatile species that remains in solution is referred to as solubility and varies from a few parts per million to a few percents depending on the species considered. The solubility of most gas species diminishes drastically with pressure (Figure 11.2). This also modifies the gas composition at depths, although there are complications when one wants to quantify such modification. One complication is linked to the difficulty in establishing solubility laws for the relevant species because they depend on melt composition, temperature, and oxidation state (Figure 11.2). Another complexity is linked to kinetics. Magma ascent and the associated pressure drop cause volatiles to come out of solution and concentrate in the gas phase. The amount of gas thus increases, turning the magma into bubbly foam. The

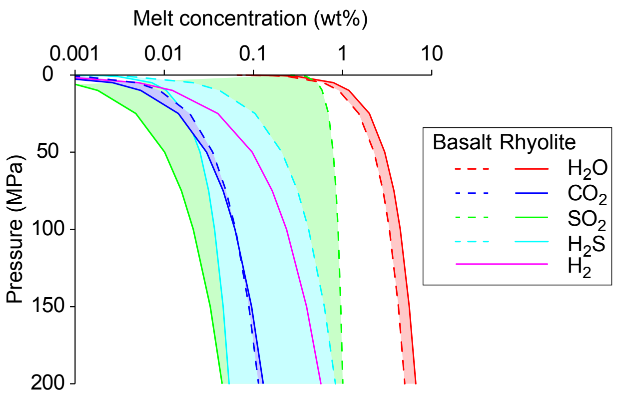

FIGURE 11.2 Maximum dissolved concentrations of five chemical species present in volcanic gases. Curves define the maximum values (solubilities) of each species taken individually. When several species are present, as in natural magmas, the melt can accommodate less of each respective species than the solubilities calculated here. Note that H_2O, H_2, and CO_2 are much less sensitive to melt composition than are sulfur-bearing species. Basaltic melt is at 1000 °C and rhyolitic melt is at 850 °C.

reactions involved, however, are much more sluggish than those occurring into the gas phase because the dissolved volatiles have to migrate (or diffuse) through the melt to reach the bubbles. Depending on the eruption style, some or all volatiles may not be able to keep up with the decompression rate and remain concentrated into the melt to values above that of solubility. These complexities make the prediction of the gas composition during ascent difficult. One method used on basaltic magmas to track the loss of volatile species during ascent is to measure their abundances in small melt pockets trapped in crystals called melt inclusions. Another method that is also valid on a restricted range of magma compositions is thermodynamical modeling.

Water being the dominant gaseous and dissolved species, it is often considered that the physics of degassing is controlled by how water degases during ascent. One exception is the degassing of CO_2-rich basalts, which is a little explored case because of experimental difficulties. Water also changes melt density much more than do other volatiles. A change in 1 wt% dissolved water in a basalt has the same effect as a temperature increase of 400 °C or a pressure decrease of 500 MPa at a constant melt water content.

2.2. Gas Bubbles

As seen in the section above, water is the dominant volcanic gas. Bubbles are thus mainly filled with water molecules and we ignore the presence of other volatiles in describing the physics of bubble nucleation, growth, **coalescence**, and collapse.

Bubbles do not appear as soon as the pressure drops below the **saturation** value. Creating a small nucleus of gas molecules takes energy, and thus, new bubbles nucleate only with a certain amount of oversaturation, which is generally measured as a pressure difference. In the simplest case, the magma is devoid of crystals, and thus, bubbles nucleate in a pure melt. Such nucleation is referred to as homogeneous and is well understood. Nucleation rate depends on water diffusivity, temperature, surface tension, and amount of oversaturation. Typically, a rhyolitic melt at saturation at 200 MPa needs to be decompressed by 120–150 MPa to nucleate bubbles homogeneously. In an ascending magma, these variables can be combined such that the bubble number density (i.e., the number of bubbles per cubic meter) can be related to decompression rate. The faster the decompression is, the more bubbles nucleate in a given volume. When the magma contains crystals, bubbles may be able to nucleate preferentially on the sides of some crystals and heterogeneous nucleation occurs. This tendency is measured by surface tension and depends on mineral species. Some minerals such as plagioclase do not modify nucleation dynamics while others, such as pyroxenes, or Fe–Ti oxides bring the necessary oversaturation from >100 MPa to values as low as 1–5 MPa. The link between bubble number density and decompression rate is maintained only if enough crystals are present. In other words, if there are not as many crystals present as the number of bubbles that would like to nucleate, one cannot predict the resulting bubble number density.

As in the case of nucleation, bubble growth is chiefly caused by the loss of pressure linked to magma ascent. Growth occurs for two distinct reasons: First, the gas expands following, to first order, the ideal gas law, and second, the amount of gas contained into the bubbles increases as pressure drops because the volatiles dissolved into the melt come out of solution (Figure 11.3). Bubbles, however, cannot grow freely because they have to push away from

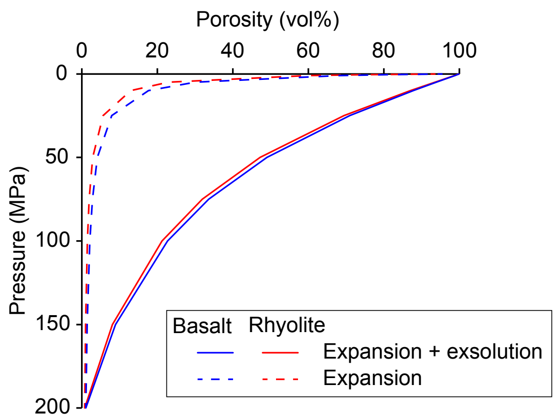

FIGURE 11.3 Evolution of magma porosity as a function of pressure. All curves start with 1 vol.% porosity at 200 MPa and bubbles are assumed to remain with the melt at all pressures (i.e., the system is closed with respect to gas). Dashed curves only take into account gas expansion, and solid curves take into account both gas expansion and exsolution. The basaltic melt is at 1000 °C and rhyolitic melt is at 850 °C. The difference between basalt and rhyolite is essentially due to temperature.

their centers the surrounding melt, crystals, and other bubbles. Leaving aside crystals and other bubbles, the simplest case is one single bubble growing in a silicate melt. At rest, the bubble internal pressure is slightly higher than the pressure of the surrounding melt because maintaining the bubble wall spherical takes some force. This force is a function of surface tension and is proportional to the bubble radius. When pressure drops because of magma ascent, the bubble walls have to push the melt away, which takes a force proportional to melt viscosity. Simultaneously, the dissolved water migrates through the melt into the bubble at a rate proportional to water diffusivity and bubble surface. The faster the pressure drops, the harder it is to work against melt viscosity and the less time water has to diffuse into the bubbles. Growth is thus a function of pressure, decompression rate, bubble size, water diffusivity, and melt viscosity. Each of the processes involved can be described by a representative timescale: τ_{dec} that quantifies decompression rate, τ_{visc} that quantifies melt flow induced by bubble growth, and τ_{diff} that quantifies diffusion of volatiles into the bubble. The relative importance of the processes is assessed by comparing these timescales. This is done by rearranging them into two dimensionless numbers that assess how important viscosity ($\Theta_V = \tau_{visc}/\tau_{dec}$) and diffusion ($\Theta_D = \tau_{diff}/\tau_{dec}$) are compared to decompression rate. If decompression dominates, bubbles grow in equilibrium, that is, bubbles stop growing as soon as decompression stops. If either viscosity or diffusion dominates, growth occurs in disequilibrium, that is, bubbles continue growing after decompression stops because their internal pressure is still much higher than the melt pressure. Disequilibrium growth thus generates overpressurized bubbles compared to the melt. This is important because this is one way to fragment the magma and generate an explosive eruption. Typically, a bubble growing from small to large has a diagonal path in a Θ_V vs Θ_D diagram (Figure 11.4). Overpressurized bubbles are thus most likely to occur when bubbles are large and decompression rates are fast.

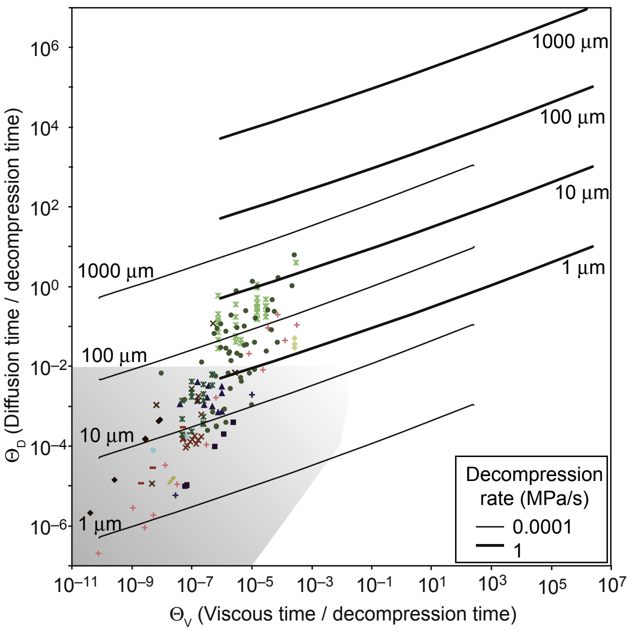

FIGURE 11.4 Bubble growth regimes as characterized by two dimensionless parameters Θ_D and Θ_V. The solid lines indicate trajectories of bubbles of a size given by the labels when they decompress from 200 MPa (lower left) to 0.1 MPa (upper right). Two decompression rates are represented, which correspond to typical effusive rates (0.0001 MPa/s) and extreme explosive rates (1 MPa/s). The melt is a rhyolite at 850 °C with a viscosity evolution with pressure shown in Figure 11.6. The gray area covers the equilibrium growth regime, whereas the area left blank characterizes disequilibrium growth. The limit between these regimes is model dependent and is symbolized by the gradient from gray to white. Symbols represent data from 14 experimental decompression studies on natural melts carried out from 1994 to 2011.

As bubbles grow, their crowding increases the likelihood that they interact with each other and merge into one another. Depending on melt viscosity, merging, or coalescence, can occur for different reasons. In low-viscosity melts, such as basalts, bubbles can rise faster than the surrounding melt. Coalescence is then driven by the differential rise speed of bubbles or, if bubbles are trapped and close packed, by gravity-driven drainage of the melt film confined between two neighboring bubbles. The new bubble quickly recovers a spherical shape. If this process involves enough parent bubbles, the resulting bubble can reach several meters in diameter at shallow depths. Its rise is then fully decoupled from that of the magma, and it can rapidly reach the surface before bursting. In higher viscosity melts, such as rhyolites, bubbles do not move relatively to each other, and coalescence occurs because of the rupture of the melt films. The exact mechanisms are still under investigation but involve shear, differential inner bubble pressure, and growth rate. Coalescence is promoted when bubbles are so crowded that they deform and create a flat melt film between each other. The coalesced bubbles keep the shape of the original bubbles for a sufficient time that bubble chains are created as more bubbles join the coalesced cluster. This process creates an interconnected network of bubbles through which the gas can flow freely; the magma is then permeable to gas.

If the gas is able to escape from the interconnected bubbles, the foamy magma collapses. As a result, the gas leaks gently out of the magma without fragmenting. Studies carried out on the mechanisms ruling bubble collapse are recent. They show that the rate at which gas is lost is controlled by **permeability**, melt viscosity, and the differential stress applied to the foam. If the magma is subjected to a sufficient pressure increase, the gas dissolves back into the melt and bubbles disappear, leaving the melt fully healed and homogeneous.

Natural observations regarding bubbles have been obtained through textural analyses of eruptive products and thanks to geophysical methods such as infrasound

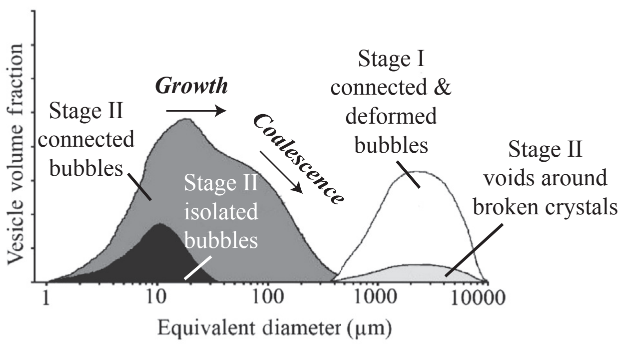

FIGURE 11.5 Schematic vesicle size distribution from explosive products of the 1997 Vulcanian explosions at Soufrière Hills volcano, Montserrat. Four vesicle populations can be identified based on size and shape. One population was generated during the first stage of degassing linked to the magma ascent from chamber to conduit (Stage I). The other populations were generated during the sudden evacuation of the conduit that fed the Vulcanian explosions (Stage II). The arrows indicate the respective effects of growth and coalescence. *Modified from Giachetti et al. (2010).*

surveying of bubble bursting during Strombolian explosions. Textural analyses give quantities such as **vesicularity**, bubble number density, and bubble size and shape, which can be linked to the various stages of bubble evolution. Briefly, nucleation controls bubble number density, growth changes bubble size and magma vesicularity, coalescence modifies bubble shape and reduces bubble number density, and collapse reduces bubble size and vesicularity. Figure 11.5 shows a schematic bubble size distribution from Vulcanian eruptive products where a few of these stages have been identified.

2.3. Crystallization

Decompression-driven water loss affects the phase equilibrium of the ascending magma. The less water is dissolved in the melt, the larger is the stability field of most anhydrous crystalline phases. In other words, water loss promotes crystallization of phases such as plagioclase, pyroxenes, and Fe−Ti oxides while destabilizing phases such as hornblende. Crystallization occurs by enlarging existing crystals and nucleating new ones. Existing crystals are often large (hundreds of micrometers across) and inherited from the magmatic chamber. Decompression-driven crystallization adds a growth rim on such crystals, which are named phenocrysts because of their size. New crystals are named microlites. They are numerous and small (tens of micrometers across) because growth time is restricted between ascent and quench at the surface.

Travel time between the chamber and the surface is too short to dissolve entire phenocrysts. Instead, they undergo fast phase transformation starting at their rims. Crystal rims break down into other water-poor phases that are stable at a low melt water content. The rate of such a reaction has been quantified experimentally and has first been used to link amphibole breakdown rate to ascent rate during the 1980 eruptions of the Mt St Helens dacite. Travel times also affect the way microlites grow. As a result, explosive products contain fewer microlites than do effusive ones.

Numerous experiments have reproduced microlite crystallization in high silica melts. General relationships can be drawn between water content and microlite volume fraction. Number densities and microlite shape, however, are controlled by kinetics, the details of which are still under investigation. Order of magnitude growth rate has been measured experimentally (10^{-11}–10^{-7} mm/s). As in cooling-driven crystallization, fast decompression triggers the fast growth of dendritic microlites while slow decompression generates more blocky shapes. The microlites found in natural products are, however, difficult to reproduce experimentally. It seems that this is due to multiple cycles of decompression and stalling in the conduit. At low pressure and low water content, which are conditions prevailing in lava domes, silica precipitation can occur. Its density is lower than that of the melt, which enables it to fill preexisting **vesicles**, possibly sealing gas pathways and stopping outgassing.

Because of experimental difficulties, microlite crystallization in basaltic melt is not well constrained. Field samples of Plinian basaltic eruptions show that up to 30 vol % microlite may be created during fast ascent and degassing, while recent experiments indicate rates on the order of 10^{-4}–10^{-5} mm/s.

3. LARGE-SCALE PROCESSES

3.1. Magma Rheology

Rheology studies address the way magma deforms when under stress. It is perhaps the domain where the unstable nature of the mixture of liquid, crystals, and gas bubbles takes its fullest meaning. As seen below, the three phases composing magma have each a distinct influence on rheology.

Melt viscosity is a function of melt composition, which includes the amount of dissolved volatiles. Water and fluorine are the two volatiles that influence most melt viscosity, the effect of water being dominant. As the amount of dissolved water decreases because of magma ascent in the volcanic conduit, melt viscosity increases by several orders of magnitude. This increase is so large that it dominates rheological changes during decompression. At low shear rates, melt viscosity is Newtonian, that is, it deforms linearly with the applied stress. As shear rate increases, however, the melt becomes viscoelastic and finally breaks. This implies that pure silicate melt fragments under sufficient shear rate. Experiments have shown that these rates too depend on melt composition through a linear dependence on viscosity; at magmatic temperatures, silica-rich melts such as rhyolites break under shear rates on the order of 10^{-2}–10^{4} s^{-1}, whereas silica-poor melts such as basalt break under rates on the order of 10^4–10^8 s^{-1}. As explained below, conduit flow models predict that the lower end of these shear rates are achievable either at the conduit margin or during the decompression-driven acceleration that occurs at shallow levels. Strain rates deduced from mass flux and conduit diameter from dome-building eruption at Montserrat and Unzen are on the order of 10^{-6}–10^{-2} s^{-1}. Despite being in the brittle range of shear rates, the melt involved into these two effusive eruptions reaches the surface unfragmented. It is thus possible for the melt to break during ascent without explosive fragmentation; after having accommodated the strain and lowered the strain rate it is subjected to, the fracture heals and the melt flows again as a Newtonian fluid.

When crystals are present in the melt, they influence the rheology in two ways: first, the larger the crystal volume fraction is, the harder it is to deform magma. In other words, the rheology of magma is a strong function of crystal volume fraction. Second, the more elongated the crystals are, the more the suspension resists deformation. Since fast-growing, ascent-related microlites are highly elongated, they influence magma rheology even when a small amount crystallizes. The details of the relationship between crystal shape and rheology is a complex issue—if microlite is platy and of the same size, it may align under deformation and instead ease motion. At high crystal volume fraction, transient shear localization occurs, that is, preferential planes of motion are constantly created and abandoned within the deformed suspension. At a still higher volume fraction, a rheological threshold is reached, and the mixture resists nonbrittle deformation. One popular way to approach these complexities is to treat melt and crystals as a perfectly homogeneous mixture with a bulk rheology. Figure 11.6 presents the simplest case of such an approach, where the bulk behavior of the mixture is assumed to be Newtonian. This approach has recently been extended to non-Newtonian behavior. A number of rheological models link together the non-Newtonian equivalent of viscosity to crystal volume fraction, crystal shape, and shear rate.

Bubbles can play a role similar to that of crystals if they remain spherical at all times, which tends to occur at low shear rates. Such rigid behavior increases bulk viscosity to a lesser degree than in the case of crystals because of the internal motion of the gas within the bubbles. At high shear rates, however, bubbles deform and ease flowage. The situation becomes quickly complex as high shear and deformation promote bubble coalescence and gas channeling. The common simplification is to calculate two extreme bulk viscosities, one for fully deformed bubbles and one for nondeforming spheres (Figure 11.6).

When the three phases are together, experiments have shown that shear localization and complex rheological response occur. Field studies have brought corroborating observations. Pyroclasts and dissected lava domes feature

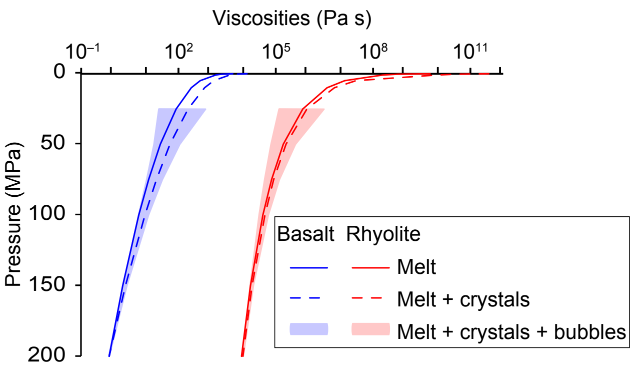

FIGURE 11.6 Evolution of magma bulk viscosities as a function of pressure. Solid curves consider melt viscosity alone and show the effect of water loss. Dashed curves add the effect of microlites, which are assumed to grow linearly from 0 to 30 vol.% for basalt and exponentially from 3 to 60 vol.% for rhyolite. Colored areas cover the two limit cases when taking gas bubbles into account, which correspond to deformable bubbles and rigid bubbles, respectively. Bubble calculations are stopped when porosity exceeds approximately 65 vol.% because foam rheology changes fundamentally above that value. Basaltic melt is at 1000 °C and rhyolitic melt is at 850 °C. Bubble volume fractions are calculated as in Figure 11.3.

shear bands of various types (alternating microlite content, melt water content, and crystal orientations) that document such phase reorganization. Figure 11.6 takes a broad stance to show that, overall, water loss and crystallization during ascent both conspire to increase magma viscosity, yielding a highly viscous lava to emerge at the surface.

3.2. Geometry of Conduit

Studies of conduit geometry brought forth a puzzling fact. Dissected volcanoes show that at a depth, magma moves preferentially along dikes and sills, that is, vertical or horizontal fracture planes that enlarge to yield a way to magma. Most volcanoes, however, erupt through vents that are shaped like vertical cylinders. There is thus a transition between shallow cylindrical conduits and deeper penny-shaped dikes.

Generally, plumbing systems of basaltic volcanoes (i.e., edifices mostly erupting fluid lavas) are composed of a series of interconnected dikes and sills feeding a central vent and several adventive vents. In such a geometrical context, experiments have shown that horizontal plumbing elements such as sills may act as bubble traps. Sills may accumulate bubbles until the foam formed collapses into a large bubble that rises rapidly to the upper reaches of the plumbing system. This mechanism drives intermittent explosions of the Strombolian type. Such conduits can be filled with magma and open to the surface for decades to millennia, as exemplified by long-lived lava lakes such as Erebus, Antarctica, and by continuously erupting volcanoes such as Stromboli, Italy. Field studies of regions with older, partially eroded, central volcanoes have shown two types of sheet-like conduits: series of regional, subvertical, and thick dikes that may span an area much larger that a single volcanic edifice, and series of local, inclined, and thin sheets. A few of these magma pathways lead to the surface.

Conduits feeding more silicic volcanoes seem to involve fewer interconnected pathways. While dikes have also been observed to dominate at a depth, the development of shallow cylindrical pipes is promoted by mechanical erosion during explosive phases. This seems to be also valid for lava dome eruptions, which commonly start by phreatic and phreatomagmatic explosions that excavate near-surface, axisymmetric vents. Not all conduits feeding silicic eruptions, however, are vertical. Localization of seismic signals at Unzen volcano, Japan, has mapped out a several-kilometer-long magmatic pathway that is inclined at 30–40° with respect to the vertical. Conduit geometry is much more complex for large-scale eruptions involving caldera formation. Caldera collapse often creates a ring fracture trough which magma is expelled. This shape breaks down if the caldera floor subsides chaotically.

The horizontal area of the conduit greatly influences how much magma can erupt. For a given decompression rate, the simplest approximation of ascent dynamics, Poiseuille's law, states that the flux of magma rising (in mass or volume per second) is proportional to the square of conduit horizontal area. In the case of a cylindrical conduit, this relationship means that the ascent rate is proportional to the square of the conduit radius. One consequence is that changes in conduit shape during eruption by erosion, transition from fissure-fed to conduit-fed, or caldera collapse, have major effects on ascent speed and thus eruptive dynamics.

An open conduit is an unstable structure that eventually collapses if empty. During an explosive eruption, there is a sharp decompression near the fragmentation level that brings a part of the conduit to pressures inferior to those of the surrounding rocks. This underpressure might induce collapse of the conduit walls and eruption shutdown. When the eruption is over, a significant part of the conduit might be left empty, which also induces an underpressure and wall collapse.

3.3. Outgassing and Permeability

During magma ascent, segregation of the gas phase from the magma, also called outgassing, occurs. This can happen through (1) buoyant bubble rise, (2) the development of a permeable bubble and fracture network, and (3) magma fragmentation.

In the case of low-viscosity magma, bubbles are able to rise buoyantly through the magma. When gas volume fraction and bubble sizes are small enough, bubbles rise together with the magma to form either a lava lake where they will follow the convective flow of the magma or a lava flow where they ooze out at low flow rates together with the magma. Larger bubbles can make their way up in the conduit individually and burst at the surface where they release gas to the atmosphere. If gas volume fraction is high enough, individual bubbles can coalesce to form large gas pockets called slugs. Slugs can fill up almost the entire width of the conduit. The bursting of these gas slugs near the surface is characteristic of Strombolian type eruptions. Even further increase in gas volume fraction might lead to annular flow, i.e. gas with particles in suspension, which has been proposed to cause Hawaiian-style fire fountain eruptions.

Bubbles in high-viscosity magmas have low mobility and remain coupled to the magma at all times. The magma–bubble mixture will therefore move as a single fluid. Unlike the case of low-viscosity magma, when bubbles coalesce, they form a permeable network, and the magma can develop a foamy structure. If the bubbles are able to connect to the surface or to the conduit walls, the gas is able to move at a different velocity compared to that of the magma, which causes low ascent rates. Such permeable pathways through which gas escapes might also be formed by fractures that develop due to friction. This friction, or shear rate, is the highest near the conduit walls and can lead to melt fracturing, which aids the gas escape to the surface. Such behavior is associated to dome-forming eruptions and coulees.

If gas and magma remain coupled, rapid ascent occurs, regardless of melt viscosity. As the gas cannot separate from the flow, the gas phase will continue to expand, pressurizing the magma and accelerating the magma–bubble mixture. This positive feedback continues until the stresses within the magma become so high that it fragments into parcels of magma called pyroclasts, which are then carried upward by the gas to the Earth's surface. The reader is referred to the chapter 25 (Volume 1) on magma fragmentation for a presentation of the different fragmentation mechanisms. Depending on the efficiency of fragmentation, this type of outgassing can result in behavior ranging from fire fountaining (usually associated with low viscous magmas) to the most violent type of explosive eruption, so-called Plinian eruptions (usually associated with more viscous magmas). The pyroclasts produced by these explosive eruptions can partially preserve the state of the magma at fragmentation and have thus been used to gain an insight into outgassing behavior. In particular, analysis of the bubble textures contained within pyroclasts has been linked to the development of permeability during magma ascent. The dominant control on permeability is vesicularity and the radius of the permeable pathways, which is related to the size and number density of bubbles. Another effect is the shape of these pathways, which is controlled by the deformation the bubbles have been subjected too. Highly deformed, large bubbles have the most favorable shape to develop high permeability.

3.4. Interactions between Conduit and Edifice

When the magma is highly viscous, it does not flow easily along conduit walls. This interaction has several consequences. First, slipping can occur at the interface. Such slipping is intermittent because it suddenly releases stress and some time is needed for new stress buildup. This is the mechanism proposed to explain sudden lava dome motions such as at Santiaguito volcano, Guatemala (Figure 11.7). The lava dome moves up several times a day in a stick-slip fashion, generating explosive events with accompanying ejecta-laden plumes. Second, the walls deform elastically under the stress imposed by the ascending magma. The elastic energy stored temporarily by the wall rock is released as soon as the dynamic pressure of the magma diminishes. This feedback mechanism influences ascent dynamics, and the resulting edifice deformations can be captured by geophysical tools such as tiltmeters or differential global positioning system measurements.

In some cases, changes of the stress field in the edifice can influence ascent dynamics. Arenal volcano, Costa Rica, has been in continuous eruption since 1968. Its conduit is open to the surface and gives way to lava extrusions and ash emissions. The conduit at Arenal is extremely sensitive to changes in stress field, as its eruptive activity can be linked to Earth's tides. Such effects, however, seem to be confined to small changes in eruptive activity rather than acting as major controls of ascent dynamics.

Shallow degassing is not confined to the magmatic column. In many instances, the volcanic gas can flow out of the column through the conduit walls. The ascending magma becomes permeable to gas when bubble networks are formed. The resulting outgassing may leak through the wall rock. Such a gas leak has been calculated to be efficient enough to reduce magma porosity and turn an explosive eruption into an effusive one. While gas leakage through conduit walls is difficult to measure, there are geological evidences of such interactions. Studies of fossil conduits have shown the presence of tuffisite veins along the magma/wallrock interface (Figure 11.8). These veins are filled with magma fragments that are less than a millimeter across and that form sedimentary structures including planar and crossbedding. Tuffisite veins are interpreted as shear fractures formed by the brittle response of highly viscous magma to flow-related shear in the conduit. The magma fragments produced during shear were redeposited through the fracture system by a gas—particle mixture, the gas phase of which was probably derived from magma outgassing.

4. PROCESS INTERACTIONS

4.1. Conduit Flow Models

Direct observations of volcanic conduits during eruptions are not possible, and therefore, numerical models are used to understand the wide variety of eruption styles at volcanoes. Modeling of magma ascent requires integrating the small- and large-scale processes that were discussed above. Each of these presents interesting and sometimes complicated physics. Conduit modeling looks at the feedbacks that occur between these processes, which present additional difficulties. We therefore rely on assumptions that reduce the complexity of the problem in order to develop such models.

The simplest approach is to present a basic conduit model that can be used to study, to a first order, the conduit dynamics during an explosive eruption. This reduces the complexities of magma ascent to a one-dimensional steady flow through a cylindrical and vertical conduit with a constant radius. The temperature of the magma does not change during ascent, the volatile phase in the magma is only made out of water, and bubbles grow at their equilibrium rate. Near the conduit inlet, at depths, the magma is considered as a homogeneous and compressible fluid made

FIGURE 11.7 Rapid uplift of Santiaguito lava dome, Guatemala with accompanying degassing and ash emission. Such explosions last tens of seconds and repeat several tens of times a day. They are inferred to be triggered by a sudden slip at the magma/wallrock interface. *Reproduced from Johnson et al. (2008).*

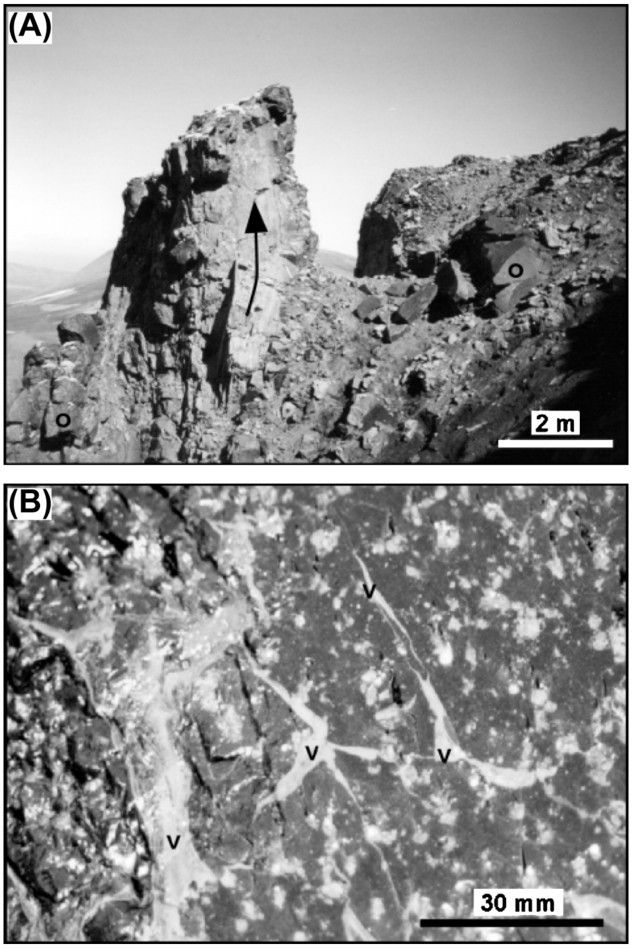

FIGURE 11.8 Eroded volcanic conduit in southeast Rauðufossafjöll, Iceland. (A) Overview of the conduit, showing dark gray obsidian walls (o) and near-vertical flow banding in the devitrified interior (arrow). (B) Network of angular, branching, pale gray tuffisite veins (v) in conduit–wall obsidian. Pale blobs are feldspar phenocrysts. *Modified from Tuffen et al. (2003).*

of a perfect mixture of melt and bubbles. The viscosity of this mixture is assumed to depend solely on melt properties, which includes melt water content. The presence of crystals is thus ignored. Fragmentation is postulated to occur when the gas volume fraction reaches a critical value. After fragmentation, the ascending magma becomes a fluid made up of a perfect mixture of gas and pyroclasts in suspension.

These assumptions can be used to write down the governing equations of the flow. The conservation of mass is

$$\frac{d(\rho u)}{dz} = 0,$$

where z is the vertical coordinate, ρ is the mixture density, and u is the ascent velocity. This equation stipulates that there is no mass gained or lost during ascent and thus that mass flow rate $q = \rho \times u$ (kg/s) during ascent remains constant. The conservation of momentum is

$$\rho u \frac{du}{dz} = -\frac{dP}{dz} - \rho g - F,$$

where P is the pressure of the magma–bubble mixture, g is the gravitational acceleration, and F is the friction force. The term on the left-hand side quantifies how the momentum changes during ascent. The three terms on the right-hand side state that momentum changes are due to (1) decompression of the magma, (2) gravitational forces, and (3) friction due to interaction with the wall, respectively.

These two equations need to be completed by defining the magma density ρ and the friction term F. The mixture density is defined as the volume average of the melt and the gas phase:

$$\rho = (1 - \varphi)\rho_m + \varphi\rho_g,$$

where φ is the gas volume fraction, ρ_m is the melt density, and ρ_g is the gas density. The melt is incompressible, and thus, its density will not change during ascent. The gas phase is compressible, and its volume expands as the pressure drops. The simplest approach is to consider that the gas phase behaves as an ideal gas.

The gas volume fraction is controlled by how much gas is exsolved at each point during ascent (Figure 11.3). Equilibrium bubble growth means that the amount of gas follows the solubility curve of water (Figure 11.2). As a first approximation, the solubility curve is described by Henry's law:

$$m_{H_2O} = s\sqrt{P},$$

where m_{H_2O} is the mass fraction of the dissolved water in the magma and s is an experimental saturation constant. This in turn can be related to the mass fraction of water that is exsolved in the mixture through the equation of mass conservation of water

$$m_{H_2O,0} = m_{H_2O,m}\left(1 - m_g\right) + m_g$$

with $m_{H_2O,0}$ being the initial mass fraction of water before exsolution and m_g the gas mass fraction within the mixture. Note that m_g is considered to be zero when $m_{H_2O,0} < m_{H_2O}$. These last three equations can be combined to calculate the gas volume fraction:

$$\frac{1}{\rho} = \frac{1 - m_g}{\rho_m} + \frac{m_g}{\rho_g},$$

$$\varphi = \frac{\rho m_g}{\rho_g}.$$

The friction term F depends on whether the magma is fragmented or not. The simplest fragmentation criterion is a critical gas volume fraction, φ_c. When the gas volume fraction is below this point, the friction with the conduit wall is governed by the magma and is thus that of a viscous flow in a pipe. Above this critical gas volume fraction, the friction with the wall is governed by the gas phase and is that of a turbulent flow in a pipe. The wall friction term can thus be written using classical works of fluid dynamics addressing viscous and turbulent flows in a circular pipe:

$$F = \frac{8\mu u}{r^2} \quad \text{if } \phi \leq \phi_c,$$

$$F = \frac{0.01u^2}{4r} \quad \text{if } \phi > \phi_c,$$

where μ is the magma−bubble mixture viscosity and r is the conduit radius. For silicic magmas, μ is calculated thanks to an experimentally derived expression that relates viscosity to the temperature and volatile content (Figure 11.6). The transition from viscous to turbulent flow is a defining feature of an explosive eruption. It causes the friction term F to become very small, which allows the velocity to increase tremendously once fragmentation occurs.

The unknowns in the above set of equations are the velocity u and the pressure P. These quantities can be solved using these equations with inflow and outflow conditions at the conduit extremities. At the inlet of the conduit, the pressure can be assumed to be equal to the pressure of the magma chamber P_0. At the outlet of the conduit, one might expect the pressure to reach the atmospheric pressure. However, when fragmentation occurs, the gas−pyroclast mixture can accelerate to high velocities. It can reach but not exceed the sound velocity of the mixture at the vent. This is called the choking condition and it fixes the value of u at the vent, regardless of conduit dimensions and magma viscosity. This condition implies that the exit pressure at the vent is larger than the atmospheric pressure, which results in a dramatic expansion at the conduit exit that generates shock waves. The solutions of these equations depend on the values of the conduit geometry (length z, radius r) and magma properties (volatile content, temperature). Parameters s and g are constant.

The dynamics of magma ascent in the conduit during an explosive eruption change dramatically. Figure 11.9 presents model solutions involving a rhyolitic melt. Initially, the gas volume fraction is zero, and the magma consists only of melt. Once the pressure is sufficiently low, the gas starts to exsolve. The feedback between the exsolution of volatiles and pressure drop creates a run-away effect by which the magma continues to accelerate until it reaches fragmentation. After fragmentation, the friction drops by many orders of magnitude and the gas−pyroclast mixture continues to accelerate until it reaches the speed of sound of the mixture at the top of the conduit. One of the solutions in Figure 11.9 has a constant melt viscosity, whereas the other

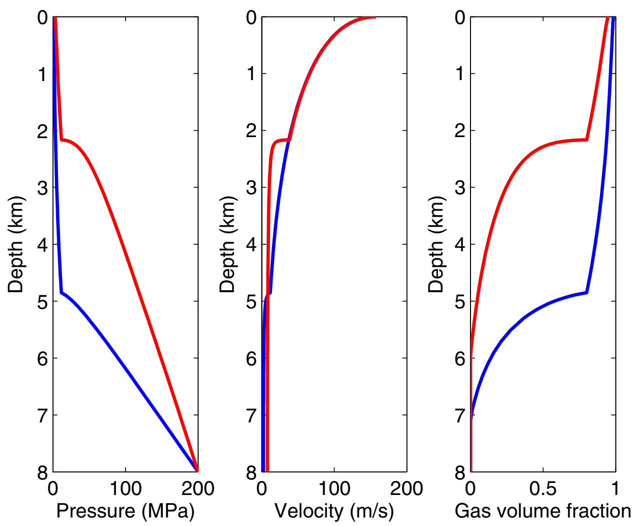

FIGURE 11.9 Results of the heuristic conduit model. Respective changes of pressure, velocity, and gas volume fraction as a function of depth in the conduit. The kinks in the profiles are generated by fragmentation and the ensuing drastic change in friction force. Blue curves represent solutions of the model using a constant melt viscosity of 10^6 Pa s. Red curves represent solutions of the model using the same empirical equation for rhyolite melt viscosity as in Figure 11.6, which depends on the magma temperature and dissolved water content. Both runs have a constant temperature of 850 °C, 5 wt.% total (and initial) water content, an inlet pressure of 200 MPa, and a conduit 8 km in length and a radius of 25 m. Following Koyaguchi (2005), a critical gas volume fraction of 0.8 is used as a fragmentation criterion.

has a viscosity that depends on melt water content. These two solutions illustrate the strong impact of melt viscosity on the depth of fragmentation.

It is clear from comparing the described model to the processes discussed in the previous sections that strong simplifications were made to arrive at a solution. In order to improve our understanding of magma ascent, the basic conduit model has been improved upon in several ways:

1. Outgassing in the basic model could only occur through magma fragmentation. In order to account for buoyant bubble rise or development of a permeable network, a two-phase model is needed such that the gas phase can move relatively to the magma. Under some conditions, such models predict solutions in which fragmentation is never reached because gas permeability allows the gas volume fraction to decrease by outgassing during ascent. These models have been predominantly used to explore the transition from effusive to explosive regimes. They have established that this transition is mostly controlled by the development of permeability relative to the wall friction.
2. Variations of magma properties across the conduit, especially rheological changes, change the velocity profile across the conduit. Such variations have been taken into account by two-dimensional models.

Permeable outgassing does not occur homogeneously within the conduit. At shallow depths, it leads to the formation of a 30- to 100-m-thick degassed magma cover at the top of the conduit and a thin blanket of degassed magma near the conduit walls.

3. Although explosive eruptions can last for hours to days, their intensity varies over time due to changes in properties that were considered constant in the simplified model (e.g., conduit radius or inlet pressure). Adding time dependence to the equations has shed light on such transient behavior. Together with outgassing and crystallization, time dependence leads to complex oscillation of the exit velocity. The strong feedback mechanisms existing between these processes greatly amplify the effect on extrusion rates of small changes of chamber pressure, conduit dimensions, or magma viscosity. When the ascent rate is such that microlite has time to crystallize, there can be multiple steady solutions for fixed conditions. Such nonlinear dynamics can cause large changes in dome extrusion rate and cyclic patterns of dome growth.

4. The shape and dimensions of the conduit are most probably not constant from chamber to vent. Some models exploring the effects of conduit shape found that the fragmentation level is typically deeper in a dyke than in a cylinder. For flows in wide dykes, the pressure at the fragmentation depth can be lower than the surrounding lithostatic pressure by several tens of megapascals, possibly leading to the collapse of the walls, which implies that this conduit geometry has a natural upper limit for dyke width. Models including a transition from dyke shape at a depth to cylindrical near the surface have shown that the fragmentation level moves into the cylindrical region, which causes the flow pressure to approach the lithostatic value and impedes wall collapse.

5. The isothermal assumption is adequate for rapid ascent. At slow ascent, however, heat loss to the conduit walls and heating due to wall friction become important mechanisms. Magma may either cool or heat up during its journey from a shallow crustal level to the volcanic vent. Cooling can be induced by heat loss at the conduit wall, or by the expansion of the gas bubbles that magma carries. Heating can be caused by latent heat release during crystallization or viscous deformation at conduit walls. Viscous heating and cooling due to gas expansion have each been calculated theoretically. Latent heat, on the other hand, has been quantified using crystal contents and mineral geothermometry of samples from explosive eruptions. It was found that these three processes can change magma temperature by up to 100 °C. To which extent these effects coexist and counteract each other in a given eruption is, however, yet unclear because of the differing methodologies employed. When these effects are accounted for, they concentrate shear in narrow zones along the conduit margin. The resulting reduction in friction drastically reduces the zone of low pressure predicted by isothermal models and moves the fragmentation level closer to the surface.

6. By assuming equilibrium exsolution, we avoided having to model bubble nucleation and growth. Delaying nucleation until oversaturation pressures of 150 MPa restricts degassing to within approximately 1500 m of the surface, which brings the fragmentation level to much shallower depths. The nucleation delay leads to higher pressures at equivalent depths in the conduit, and higher mass flux and exit pressures. The introduction of disequilibrium degassing reduces the deviation from lithostatic pressure, the flow acceleration before fragmentation, and the associated decompression rate. The presence of carbon dioxide is important in steering these dynamics as well. An increase in the proportion of carbon dioxide produces a decrease in the mass flow rate and an increase in the exit gas volume fraction and depth of the fragmentation level.

7. Unlike assumed in the simple model of Figure 11.7, the rheology of the magma depends on the presence of bubbles and crystals. Models using bulk expressions that take their effect on viscosity in account have shown that bubbles cause a decrease in calculated fragmentation depth and an increase in calculated eruption rate. Models based on non-Newtonian formulations of magma rheology have shown that shear bands are most likely to initiate at the junction of the conduit and base of the dome, where the shear stress experienced between new lava entering the dome and existing lava is the greatest.

8. The fragmentation criterion of a critical gas volume fraction is simplistic. Other criteria, such as that of a critical stress, or that of critical bubble overpressure, do not change the outputs of 1D models much because of the narrowness of the region where large decompression rates are attained. This is not true for 2D models, as different criteria lead to fragmentation occurring in different regions; critical stresses, for instance, are reached at conduit walls before being reached in the center.

4.2. Eruptive Dynamics at the Surface

Shallow magma ascent gives rise to a rich diversity of processes that cause volatile to come out of solution from a silicate melt to produce a highly expansible gas phase. The surficial expression of these processes has been broadly classified into effusive eruptions that produce lava flows and lava domes and explosive eruptions that range from short-lived explosions of the Hawaiian, Strombolian, or Vulcanian type to long-lived (sub-) Plinian eruptive columns.

There are several key parameters that control this diversity. Melt viscosity and thus magma type control bubble mobility. In low-viscosity magmas, highly mobile bubbles have time to migrate, coalesce, and escape from the magma, yielding eruptive styles combining lava flows and Hawaiian or Strombolian bubble bursts. If fast enough, ascent rate can counteract bubble mobility and yield more explosive behavior such as basaltic Plinian eruptions. In high-viscosity magmas, less mobile bubbles are constrained either to coalesce into a permeable network that allows for outgassing and lava dome formation or to accumulate until fragmentation liberates the gas phase and allows for Vulcanian or (sub-) Plinian gas and ash column to form.

The first and most complete paradigm of magma ascent and degassing is that of the Plinian eruptive regime illustrated in Figure 11.9. Similar frameworks have been then proposed for effusive regimes with outgassing and for regime where individual bubble motion predominates. Although most of these templates capture the essentials of shallow degassing processes, many mechanism descriptions still need to be refined. One example is phreatic eruptions because the links between small-scale processes involved in magma degassing in the presence of surficial water and large-scale processes involved in steam and ash generation remain unclear. These modeling efforts where fed by experimental data and natural observations and build canonical cases of eruptive regimes. In parallel, the past decade has seen the emergence of numerous observations and quantifications of lower intensity eruptive regimes. A significant fact is that the boundaries between these canonical eruptive regimes blur as more and more observations are collected. One of the many examples of such refinement is the current research effort to distinguish the subtleties between "violent Strombolian" and "Vulcanian" explosions.

FURTHER READING

Burgisser, A., Scaillet, B., 2007. Redox evolution of a degassing magma rising to the surface. Nature 445, 194−197.

Carroll, M.R., Holloway, J.R., 1994. Volatiles in magmas. In: Reviews in Mineralogy, vol. 30. Virginia.

Giachetti, T., Druitt, T.H., Burgisser, A., Arbaret, L., Galven, C., 2010. Bubble nucleation, growth and coalescence during the 1997 Vulcanian explosions of Soufrière Hills Volcano, Montserrat. Journal of Volcanology and Geothermal Research 193, 215−231.

Giordano, D., Russell, J.K., Dingwell, D.B., 2008. Viscosity of magmatic liquids: a model. Earth and Planetary Science Letters 271, 123−134.

Gonnermann, H.M., Manga, M., 2007. The fluid mechanics inside a volcano. Annual Review of Fluid Mechanics 39, 321−356.

Gonnermann, H.M., Manga, M., 2013. Dynamics of magma ascent in the volcanic conduit. In: Fagents, S.A., Gregg, T.K., Lopes, R.M.C. (Eds.), Modeling Volcanic Processes: The Physics and Mathematics of Volcanism. Cambridge University Press, Cambridge, pp. 55−84.

Hammer, J., 2008. Experimental studies of the kinetics and energetics of magma crystallization. Reviews in Mineralogy and Geochemistry 69, 9−59.

Johnson, J.B., Lees, J.M., Gerst, A., Sahagian, D., Varley, N., 2008. Long-period earthquakes and co-eruptive dome inflation seen with particle image velocimetry. Nature 456, 377−381. http://dx.doi.org/10.1038/nature07429.

Keating, G.N., Valentine, G.A., Krier, D.J., Perry, F.V., 2007. Shallow plumbing systems for small-volume basaltic volcanoes. Bulletin of Volcanology 70, 563−582.

Koyaguchi, T., 2005. An analytical study for 1-dimensional steady flow in volcanic conduits. Journal of Volcanology and Geothermal Research 143, 29−52.

Llewellin, E.W., Manga, M., 2005. Bubble suspension rheology and implications for conduit flow. Journal of Volcanology and Geothermal Research 143, 205−217.

Martel, C., 2012. Eruption dynamics inferred from microlite crystallization experiments: application to Plinian and dome-forming eruptions of Mt. Pelée (Martinique, Lesser Antilles). Journal of Petrology 53, 699−725.

Métrich, N., Wallace, P., 2008. Volatile abundances in basaltic magmas and their degassing paths tracked by melt inclusions. Reviews in Mineralogy and Geochemistry 69, 363−402.

Navon, O., Lyakhovsky, V., 1998. Vesiculation processes in silicic magmas. In: Gilbert, J.S., Sparks, R.S.J. (Eds.), The Physics of Explosive Volcanic Eruptions. Geological Society Special Publication No 145, London, pp. 27−50.

Pistone, M., Caricchi, L., Ulmer, Burlini, L., Ardia, Reusser, E., Marone, F., Arbaret, L., 2012. Deformation experiments of bubble- and crystal-bearing magmas: rheological and microstructural analysis. Journal of Geophysics Research 117, B05208. http://dx.doi.org/10.1029/2011JB008986.

Stasiuk, M.V., Barclay, J., Carroll, M.R., Jaupart, C., Ratte, J.C., Sparks, R.S.J., Tait, S.R., 1996. Degassing during magma ascent in the Mule Creek vent (USA). Bulletin of Volcanology 58, 117−130.

Tuffen, H., Dingwell, D.B., Pinkerton, H., 2003. Repeated fracture and healing of silicic magma generate flow banding and earthquakes? Geology 31, 1089−1092.

Zhang, Y., Xu, Z., Zhu, M., Wang, H., 2007. Silicate melt properties and volcanic eruptions. Reviews of Geophysics 45, RG4004. http://dx.doi.org/10.1029/2006RG000216.